

Experimental and Theoretical Study of the Reactions $C_2H_5CO + O_2$ and $CH_3CHC(O)H + O_2$

R. Nádasi¹, I. Szilágyi¹, G. L. Zügner¹, S. Dóbe^{1*}, J. Zádor^{1,3}, X. Song², B. Wang^{2*}

¹Chemical Research Center, Hungarian Academy of Sciences, Budapest, Hungary

²College of Chemistry and Molecular Sciences, Wuhan University, Wuhan, People's Republic of China

³Combustion Research Facility, Sandia National Laboratories, Livermore, USA

Abstract

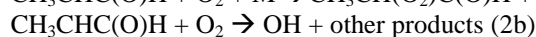
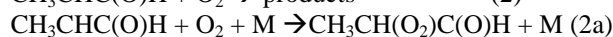
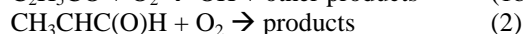
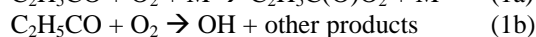
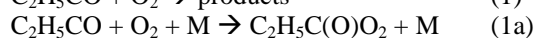
The kinetics of OH formation for the reaction $C_2H_5CO + O_2$ have been studied at 298 K using the low-pressure discharge flow technique coupled with resonance fluorescence monitoring of OH radicals. OH yields are close to unity at around 1 mbar pressure of He, but decrease strongly with increasing pressure. The experimental OH yields could be reproduced well using multichannel variational RRKM theory. Ab initio CBS-QB3 computations have been carried out to explore the potential energy surface of the reaction system $CH_3CHC(O)H + O_2$. The lowest-energy reaction path has been found to be the association step followed by 1,4 H-atom migration to form OH, CH_3CHO and CO.

1. Introduction

Oxygenated fuels (alcohols, ethers and esters) have been increasingly used as additives and even replacements for fossil fuels. They can improve combustion performance, produce less CO and particulate matter, and have the potential to offer an improved balance of CO₂ emissions. On the other hand, they exhibit a greater propensity to emit aldehydes, among them propionaldehyde, C_2H_5CHO , [1]. Aldehydes are themselves toxic and have significant ozone creating potential in the troposphere, therefore their formation and further reactions may give rise to degraded air quality.

Propionaldehyde is depleted in the troposphere via photo-oxidative chain reactions, the initiation step of which is the hydrogen abstraction reaction by OH radicals. In the initiation step, propionyl, C_2H_5CO , and to a lesser extent, 2-methyl-vinoxyl, $CH_3CHC(O)H$, radicals are formed. In view of the recent discovery that enols are common intermediates in hydrocarbon flames [2], the enol-form of propionaldehyde, $CH_3CH=C(H)OH$, is likely to be present in combusting systems besides its normally encountered keto-form. Hydrogen abstraction reactions of the keto-form propionaldehyde lead to propionyl, while those of the enol-tautomer most likely to 2-methyl-vinoxyl. These structural isomer radicals react to their greater part with O_2 both in combustion systems and under atmospheric conditions.

As part of a wider research program, the oxidation kinetics of C_2H_5CO and $CH_3CHC(O)H$ are being studied in our groups by using experimental and theoretical methods. Here we report experimental and theoretical OH yields for $C_2H_5CO + O_2$, i.e. branching ratios, $\Gamma_{1b} = k_{1b}/k_1$, at room temperature, as well as molecular mechanism for $CH_3CHC(O)H + O_2$ from quantum chemical computations.

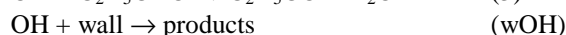
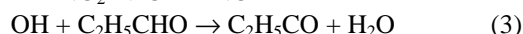
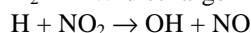


2. Methods

2.1 Experimental

The low-pressure fast discharge flow method (DF) was applied to investigate the kinetics of OH formation in the reaction of propionyl radicals with O_2 . OH radicals were detected by $A^2\Sigma(v=0) \leftarrow X^2\Pi(v=0)$ resonance fluorescence (RF) using a microwave-powered resonance lamp for excitation. Details of the kinetic apparatus and RF detection have been presented in previous publications [3–5].

Briefly, the 60.0-cm-long, 4.01-cm-i.d. flow reactor was made of Pyrex and was coaxially equipped with a moveable quartz injector. The inner surface of the reactor was coated with a thin layer of halocarbon wax to reduce heterogeneous wall effects. C_2H_5CO radicals were produced in the flow reactor by reacting OH radicals with excess propionaldehyde, while OH was obtained by reacting H atoms with a slight excess of NO_2 inside the moveable injector. Hydrogen atoms were generated by microwave-discharge dissociation of H_2 , premixed with Ar, in large excess of He (Ar served to facilitate the dissociation of H_2 amounting to $\alpha \approx 15\%$).



* Corresponding authors: 1* dobe@chemres.hu

2* baoshan@whu.edu.cn

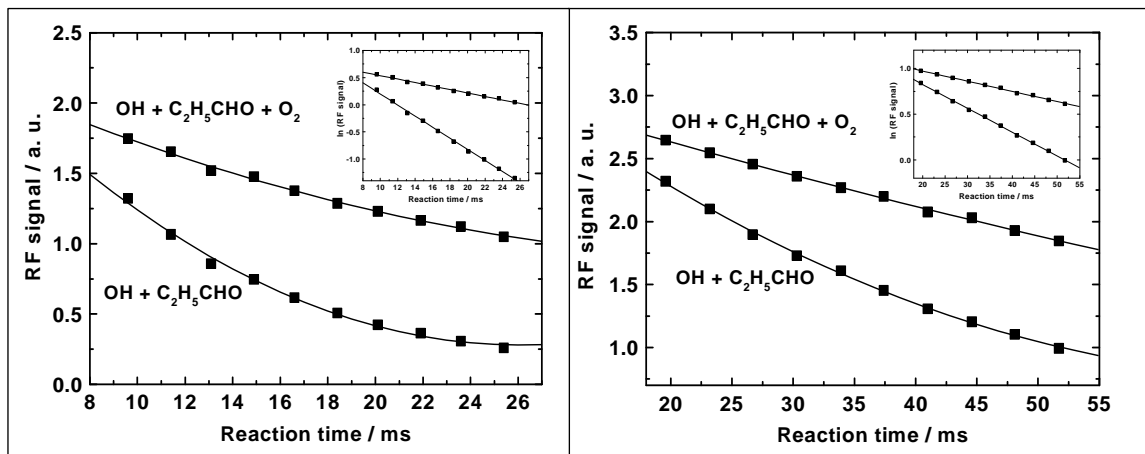


Fig.1. Representative pseudo-first-order decay profiles used to determine OH yield for the $\text{C}_2\text{H}_5\text{CO} + \text{O}_2$ reaction. The two sets of decays have been obtained applying different initial OH concentrations and with different propionaldehyde and O_2 concentrations both used in large excess.

Helium was the main carrier gas which was regulated by calibrated mass flow controllers. The smaller flows of reactants and radical-source molecules were regulated by needle valves and determined from the pressure rise over time in known volumes. The reaction pressure was measured with a calibrated capacitance manometer. The flow tube was connected downstream to a detection block where the induced resonance fluorescence of OH was viewed through an interference filter centred at 307 nm and detected by a photomultiplier. The multiplier output was fed into a purpose-built data acquisition PC-board for signal averaging and further analysis. The detection limit for OH was $\sim 2 \times 10^9$ molecule cm^{-3} (at $S/N = 1$ signal-to-noise ratio).

The experimental procedure involved monitoring of the concentration of OH radicals along the flow tube at different positions of the moveable injector in the presence and absence of O_2 , i. e., for $\text{OH} + \text{C}_2\text{H}_5\text{CHO}$ and $\text{OH} + \text{C}_2\text{H}_5\text{CHO} + \text{O}_2$. Both propionaldehyde and O_2 were used in large excess over OH and they entered the reactor upstream through side arms. Typically, the initial OH concentration was $[\text{OH}]_0 \approx 4 \times 10^{11}$ molecule cm^{-3} , along with $[\text{C}_2\text{H}_5\text{CHO}] \approx 7 \times 10^{12}$ and $[\text{O}_2] \approx 1 \times 10^{15}$ molecule cm^{-3} . The “ O_2 flow on” and “ O_2 flow off” runs, or vice versa, were conducted in a back-to-back manner. The linear flow velocity was $v_{\text{lin}} \approx 10$ m s^{-1} allowing kinetic measurements between about 2 and 50 ms reaction time.

The experiments were carried-out at room temperature, $T = 298 \pm 3$ K, in the pressure range of $P = 1.37$ – 13.34 mbar of He.

Table 1
Materials used in the experiments

Name	Supplier	Purity (%)	Notes
He	Messer-Griesheim	99.996	^a
H_2	Messer Griesheim	99.995	^b
Ar	Linde	99.9990	^b
O_2	Messer Griesheim	99.995	
NO_2	Messer Griesheim	98	^c
$\text{C}_2\text{H}_5\text{CHO}$	Fluka	> 99.5	^d

^a As a carrier gas, it was passed through liquid-nitrogen-cooled silica-gel traps before entering the flow system. ^b Used as 5% H_2 + 10% Ar mixture in He. ^c Purified by low-temperature trap-to-trap distillation in vacuum and used as 1% mixture in He. ^d Degassed by freeze-pump-thaw cycles prior to use. It was metered in the flow tube either directly or premixed in 10–15% with He.

2.2 Theory

Multichannel variational RRKM theory has been applied to estimate OH yields for the reaction $\text{C}_2\text{H}_5\text{CO} + \text{O}_2$. Input parameters were taken from our recent high level ab initio molecular orbital study performed up to full coupled cluster theory with the complete basis set (FCC/CBS) [6]. Details of the theoretical reaction kinetic computations have been presented also in [6] as well as in [7].

Ab initio CBS-QB3 computations have been carried out to characterise the potential energy surface (PES) of the reaction system $\text{CH}_3\text{CHC}(\text{O})\text{H} + \text{O}_2$. CBS-QB3 is a powerful composite method [8] comprising CCSD(T), MP4SDQ and MP2 with increasingly sophisticated basis sets. Importantly for our present subject, CBS-QB3 includes a correction for spin contamination in open shell species.

3. Results and Discussion

3.1 Experimental OH Yields for the Reaction of C₂H₅CO with O₂

A large increase in the OH signals was observed when O₂ was added to the reaction system of OH with C₂H₅CHO, and the depletion of OH became less steep. In all experiments, the time history of OH has been found to obey first-order kinetics for both OH + C₂H₅CHO and OH + C₂H₅CHO + O₂ (Fig.1). The observed kinetic behaviour is understood by the reformation of OH via the chain reactions (3) – (1a) in the presence of a large excess of of the reactants over OH radicals (Fig.2).

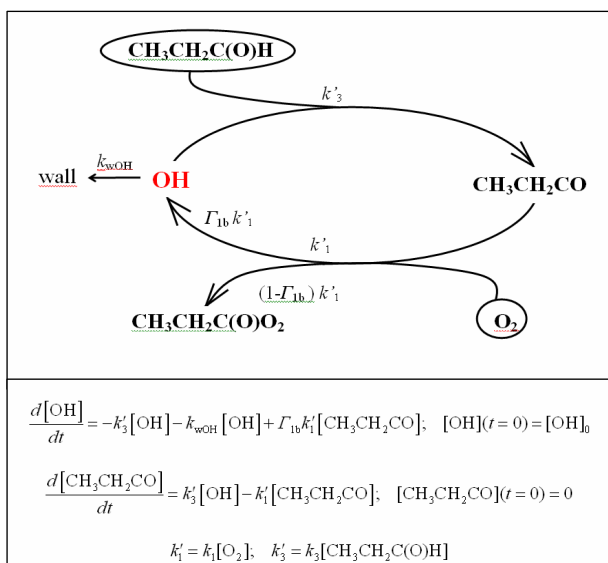


Fig.2. Reaction scheme and rate equations for the reaction system OH + C₂H₅CHO + O₂ with large excess of both propionaldehyde and oxygen molecules over the hydroxyl radicals.

A large increase in the OH signals was observed when O₂ was added to the reaction system of OH with C₂H₅CHO, and the depletion of OH became less steep. In all experiments, the time history of OH has been found to obey first-order kinetics for both OH + C₂H₅CHO and OH + C₂H₅CHO + O₂ (Fig.1). The observed kinetic behaviour is understood by the reformation of OH via the chain reactions (3)–(1a) at the high excess of the reactants over hydroxyl (Fig.2).

Under the experimental conditions applied, just about reactions (1a), (1b), (3) and (wOH) take place, the differential equation system of which can be solved analytically [9] providing equation (I) for the OH yield.

$$\Gamma_{lb} = \frac{\kappa_0 - \kappa^*}{\kappa_0 - k_{wOH}} \quad (1)$$

where κ_0 is the OH decay constant with C₂H₅CHO, κ^* is the OH decay constant with C₂H₅CHO + O₂ and k_{wOH} is the “wall rate constant”. The experimental conditions and results have been summarised in Table 2.

Table 2

Experimental OH yields, Γ_{lb} , for the reaction of C₂H₅CO radicals with O₂ ($T = 298$ K)

$P(\text{He})$ mbar	κ_0^a (s ⁻¹)	κ^*^b (s ⁻¹)	k_w^c (s ⁻¹)	Runs ^d	Γ_{lb}^e
1.37	38-176	8-42	8	10	0.88 ± 0.06
2.00	90-129	9-33	5	6	0.86 ± 0.07
2.61	20-185	2-54	5	7	0.84 ± 0.06
3.59	14-155	8-63	5	7	0.68 ± 0.05
6.22	28-169	15-84	5	9	0.62 ± 0.06
8.15	27-57	16-43	8	11	0.53 ± 0.06
10.00	21-60	14-35	4	6	0.44 ± 0.05
13.34	32-112	23-77	8	6	0.33 ± 0.05

^a OH decay constant in the absence of O₂. ^b OH decay constant in the presence of O₂. ^c Loss rate constant of OH on the wall of the reactor. ^d Number of back-to-back determinations of κ_0 and κ^* decay constants. ^e The errors refer to 1 σ precision.

3.2 Pressure Dependence of the OH Yield of C₂H₅CO + O₂

The OH yields determined in our experiments are close to unity at and around 1 mbar, but decrease strongly with pressure implying that propionyl-peroxy radical is the dominant reaction product above about 10 mbar (Fig. 3).

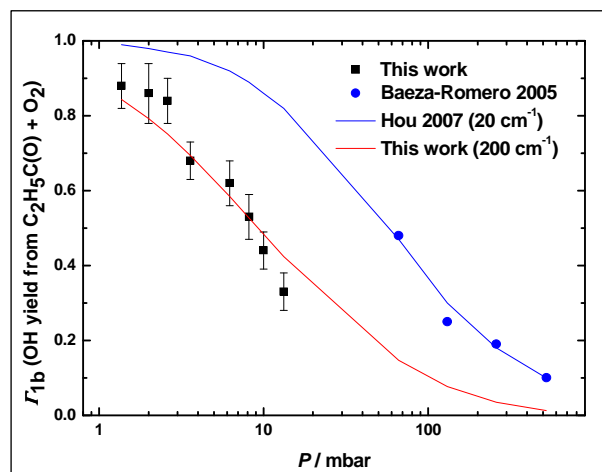


Fig.3. Comparison of OH yields for the reaction of propionyl radicals with O₂ at room temperature, in He buffer gas. The symbols are experimental data, while the curves are theoretical results obtained with different energy transfer parameters (see text).

The only other experimental study we are aware of has been performed by Baeza-Romero and co-workers [10] who used exciplex laser photolysis of diethyl-ketone as a source of C₂H₅CO radicals, at higher pressures. The results they have reported are also presented in Fig.3. As seen, the OH yields determined by the Leeds group are significantly larger and decrease more slowly with increasing pressure. Similar disparity has been observed for the OH yield of the CH₃CO + O₂ reaction [9, 11–12].

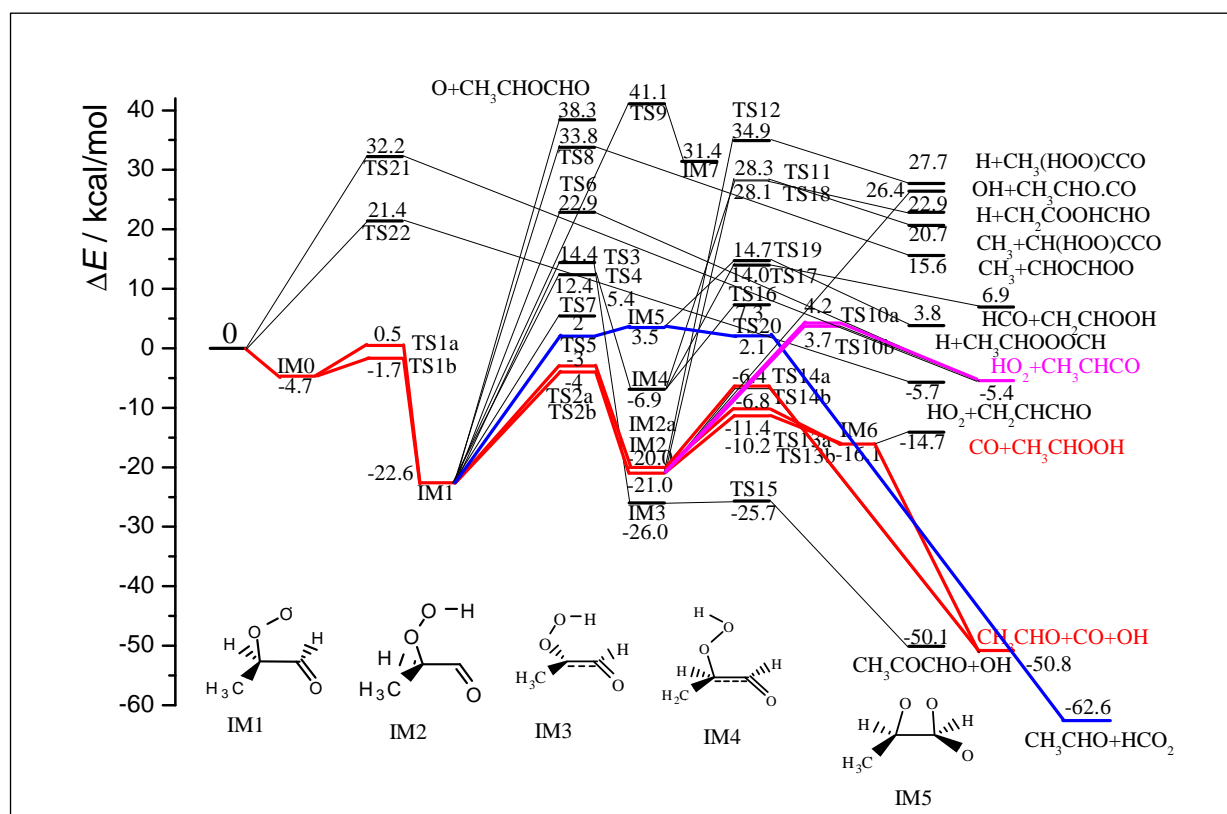


Fig.4. Energetics for the $\text{CH}_3\text{CH}(\text{O})\text{H} + \text{O}_2$ reaction calculated at the CBS-QB3 // B3LYP/6-311G(2d, d, p) level of theory. The energies are in kcal/mol and include zero-point energy corrections.

In our FCC/CBS/RRKM study, the average energy transferred per collision was chosen as a fitting parameter giving good agreement with the current experiments with $-\langle\Delta E\rangle = 200 \text{ cm}^{-1}$ (see in Fig.3). Note that $-\langle\Delta E\rangle = 138 \text{ cm}^{-1}$ ($T = 298 \text{ K}$) has been estimated for He buffer gas in case of the analogous $\text{CH}_3\text{CO} + \text{O}_2$ reaction system [7]. On the other hand, in a very similar theoretical study by Hou et al. [6], the value of $-\langle\Delta E\rangle = 20 \text{ cm}^{-1}$ has been found to reproduce well the OH-yields reported in [10] (Fig. 3).

It appears therefore that “low” energy transfer parameters are consistent with some of the experimental OH yields reported for the $\text{RCO} + \text{O}_2$ reactions, while “high” ones with others ([9], [13], and this work). Clearly, further experimental and theoretical studies are required to resolve the disagreement that exists about the kinetics of acyl radical reactions with O_2 .

3.3 Characterisation of the Potential Energy Surface of the $\text{CH}_3\text{CH}(\text{O})\text{H} + \text{O}_2$ Reaction System

44 stationary points, including transition states and reaction intermediates, have been characterised on the PES of the reaction (Fig.4). The reaction proceeds predominantly via an addition/elimination mechanism, while direct abstraction is negligible.

The association step between 2-methylvinoxyl and O_2 , occurring via a weakly-bonded complex, leads to the formation of the $\text{CH}_3\text{CH}(\text{O}_2)\text{C}(\text{O})\text{H}$ peroxy radical (IM1), which possesses $\sim 23 \text{ kcal mol}^{-1}$ excess energy. Several reaction pathways depart from the peroxy radical adduct, the lowest-energy of which is the 1,4-intramolecular hydrogen atom migration that gives rise to the hydroperoxyl-radical, $\text{CH}_3\text{CH}(\text{O}_2\text{H})\text{CO}$ (IM2). Note that the barrier for this isomerization step is below the reactants 2-methylvinoxyl + O_2 .

$\text{CH}_3\text{CH}(\text{O}_2\text{H})\text{CO}$ decomposes via consecutive steps to hydroxyl radical, acetaldehyde and CO as the final products (Fig.4).

3.4 Molecular Mechanism of the Reactions of Carbonyl Radicals with O_2

In this concluding section we have summarised some previous results, information available from the literature and our present findings for the reactions $\text{CH}_3\text{CO} + \text{O}_2$ [7], [9]; $\text{C}_2\text{H}_5\text{CO} + \text{O}_2$, [6], this work; $\text{CH}_3\text{C}(\text{O})\text{CH}_2$ (1-methyl-vinoxyl) + O_2 , [9]; $\text{CH}_3\text{CH}(\text{O})\text{H} + \text{O}_2$ (2-methylvinoxyl) + O_2 [14], this work. A schematic reaction mechanism is presented in Fig.5.

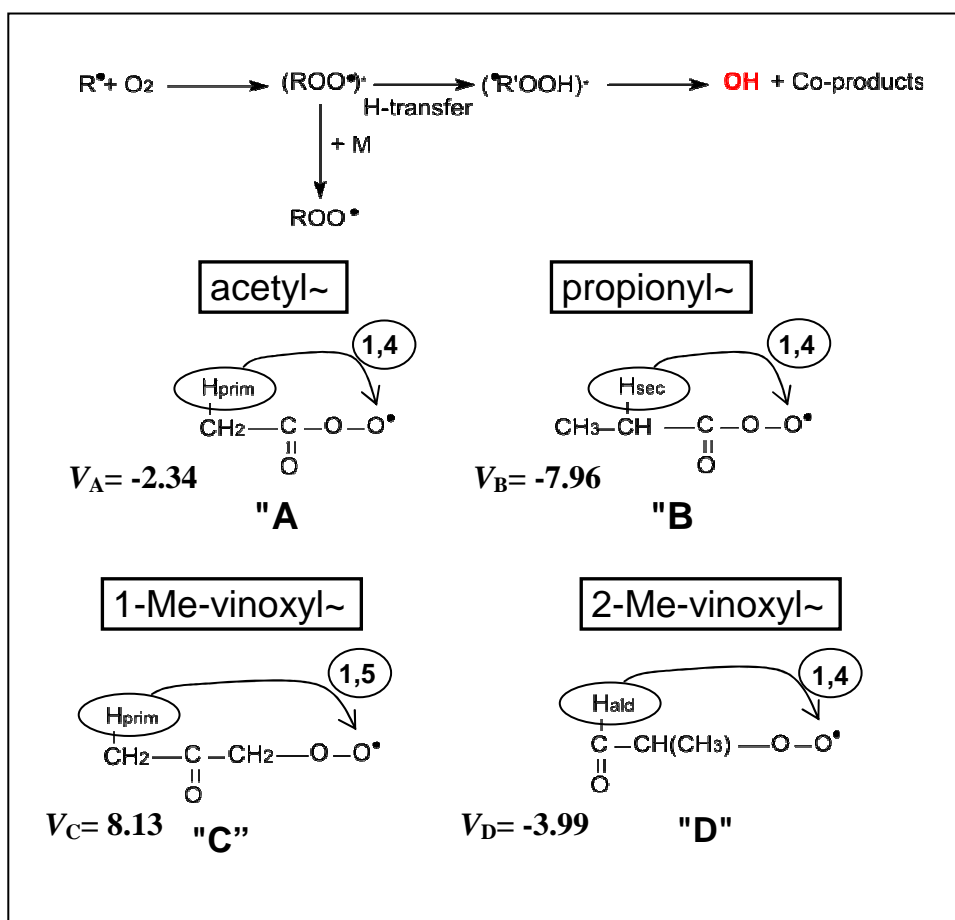


Fig.5. Comparison of the molecular mechanism for the reactions of carbonyl free radicals with O_2 by results from the present study and literature sources. V_A , V_B , etc, designate the respective barriers for the intramolecular H-transfer relative to reactants and are given in kcal mol^{-1} including ZPE correction.

All four reactions display a multi-well–multi-channel reaction mechanism. In the first, association step, vibrationally excited peroxy radicals are formed. Competition between stabilisation by collisions and reformation to reactants give rise to pressure dependence.

The peroxy radicals can undergo a series of consecutive reactions that lead to OH formation (and different co-products). The rate limiting step is the $ROO \rightarrow R'OOH$ intramolecular H atom transfer (IHT).

The significant OH yields observed for acetyl + O_2 and propionyl + O_2 are understood by that the barriers for IHT are below the energy levels of the reactants (schemes "A" and "B" in Fig.5.).

The non-finding of OH for 1-methylvinoxyl + O_2 is consistent with the substantial barrier for the IHT step, $CH_3C(O)CH_2OO \rightarrow CH_2C(O)CH_2OOH$, which may reflect some resonance stabilisation of the 1-methylvinoxyl-peroxy radical (scheme "C" in Fig.5.). In contrast with this, OH-formation is more facile for the 2-methylvinoxyl + O_2 reaction, because the low-

bond-energy carbonyl H atom is involved in IHT (scheme "D" in Fig.5.).

Acknowledgements

This work has been supported by the EU's FP6 Project SCOUT-O3 (contract GOCE-CT-2004-505390) and the Hungarian Scientific Research Fund OTKA (contract K68437).

References

- [1] X. Shia, X. Panga, Y. Mua, H. Hea, S. Shuaib, J. Wangb, H. Chenb, R. Lib, Atmos. Environ., 40 (2006) 2567.
- [2] C.A. Taatjes, N. Hansen, A. McIlroy, J.A. Miller, J.P. Senosiain, S.J. Klippenstein, F. Qi, L. Sheng, Y. Zhang, T.A. Cool, J. Wang, P.R. Westmoreland, M.E. Law, T. Kasper, K. Kohse-Höinghaus, Science, 308 (2005) 1887.
- [3] S. Dóbbé, L.A. Khachatryan, T. Bérces, Ber. Bunsenges., Phys. Chem., 93 (1989) 847.

- [4] K. Imrik, E. Farkas, G. Vasvári, S. Dóbbé, I. Szilágyi, D. Sarzynski, T. Bérces, F. Márta, *Phys. Chem. Chem. Phys.*, 6, (2004) 3958.
- [5] E. Farkas, PhD Thesis, Technical University, Budapest, 2005.
- [6] H. Hou, B. Wang, *J. Chem. Phys.*, 127 (2007) 054306.
- [7] H. Hou, A. Li, H.Y. Hu, Y. Li, H. Li, B. Wang, *J. Chem. Phys.*, 122 (2005) 224304.
- [8] J.A. Montgomery, M.J. Frisch, J.W. Ochterski, G.A. Petersson, *J. Chem. Phys.*, 110 (1999) 2822.
- [9] Gg. Kovács, J. Zádor, E. Farkas, R. Nádasdi, I. Szilágyi, S. Dóbbé, T. Bérces, F. Márta, G. Lendvay, *Phys. Chem. Chem. Phys.*, 9 (2007) 4142.
- [10] M.T. Baeza-Romero, M.A. Blitz, D.E. Heard, M.J. Pilling, B. Price, P.W. Seakins, *Chem. Phys. Lett.*, 408 (2005) 232.
- [11] M.A. Blitz, D.E. Heard, M.J. Pilling, *Chem. Phys. Letters*, 365 (2002) 374.
- [12] S.C. Carr, M.T. Baeza-Romero, M.A. Blitz, M.J. Pilling, D.E. Heard, P.W. Seakins, *Chem. Phys. Letters*, 445 (2007) 108.
- [13] A. Maranzana, J.R. Barker, G. Tonachini, *Phys. Chem. Chem. Phys.*, 9 (2007) 4129
- [14] T. Oguchi, A. Miyoshi, M. Koshi, N. Washida, *J. Phys. Chem. A*, 105 (2001) 378.